Cost-effective synthesis method of facile environment friendly SnO_2 nanoparticle for efficient photocatalytic degradation of water contaminating compound

Sucharita Chakraborty, Mouni Roy and Rajnarayan Saha

ABSTRACT

The present study demonstrates an intensive experimental work based on the tin oxide (SnO_2) nanoparticle synthesis which was successfully carried out by a simple conventional precipitation method followed by calcination at 700 °C. The synthesized nanoparticles were characterized by X-ray powder diffraction (XRD), UV–Vis spectroscopy, Fourier transform infrared spectroscopy (FTIR), field emission scanning electron microscopy (FESEM) and energy-dispersive X-ray spectroscopy (EDAX). The XRD pattern proves that tetragonal rutile structure SnO_2 nanoparticles were formed. The crystallite particle size calculation from Scherer's equation revealed the average size of 28.5 nm. The absorption spectrum of SnO_2 nanoparticles showed absorption band at about 290 nm and the band gap energy (E_g) from Tauc plot was obtained at 3.8 eV. The photocatalytic degradation of pharmaceutical compound, 4-aminopyridine (5 ppm) using synthesized SnO_2 nanoparticle, was assessed. The effect of variable catalyst dosage, pH and irradiation sources, were studied. The optimum catalyst dosage and pH were found to be 1.5 gm/L and 6.5, respectively. The degradation efficiency of water contaminant 4-aminopyridine under UV light and solar light irradiation for 120 min were found to be 97% and 11%, respectively. The reusability of the catalyst was checked and has been found stable after three photocatalytic runs.

Key words | 4-Aminopyridine, cost-effective, degradation, metal oxide nanoparticle, photocatalytic activity, precipitation method

Sucharita Chakraborty
Mouni Roy
Rajnarayan Saha (corresponding author)
Department of Chemistry,
National Institute of Technology,
Durgapur 713209, West Bengal,
India
E-mail: *rnsahanitd@gmail.com*

INTRODUCTION

Pharmaceutical, textile and chemical industries being the cradle of all scientific and technical progress imparts majorly for the advancement of human society. However, these chemicals, when they find their way to the aqueous environment, results in severe environmental pollution that negatively effects the entire ecosystem. To get rid of these toxic effluents, biodegradation was used traditionally. The cost-effectiveness and low efficacy are the major disadvantages of the biodegradation process (Li *et al.* 2018). In the field of wastewater treatment, employment of nanostructured materials has fascinated the researchers due to its outstanding physico-chemical properties (An *et al.* 2005; Ali *et al.* 2010; Al-Hamdi *et al.* 2015) which are dissimilar from the bulk state (Bagheri-Mohagheghi *et al.* 2008).

The most widely used metal oxides such as zinc oxide (ZnO) and titanium dioxide (TiO_2) with wide band gap semiconductors are used currently in the decontamination of wastewater. Quite a number of previously published works were centered on TiO_2 and ZnO for degradation of organics. Many researchers reported that TiO_2, ZnO and tin dioxide (SnO_2) are the most active catalysts for the degradation of dyes, phenols and pesticides (Al-Hamdi *et al.* 2015).

In this regard, there are few literature reports showing the study of tin oxide (SnO_2) of rutile-type crystal structure making it a topic of immense interest for the researchers. SnO_2 is a typical n-type semiconductor with a wide band gap of about 3.6 eV (Viet *et al.* 2016). This low cost material shows high electron mobility excellent optical, gas-sensing properties and chemical stability (Hu *et al.* 2017) which was widely used in sensors (Tripathy *et al.* 2013), solar cells (Hara *et al.* 2011; Chen *et al.* 2012) and lithium ion batteries

doi: 10.2166/wst.2020.130

(Lin *et al.* 2012). However, for the degradation of organic pollutants, water splitting and hydrogen production, SnO_2 has proved to be an excellent photocatalyst (Prakasha *et al.* 2016). SnO_2 is poorly absorbed by the human body when injected or inhaled (Kim *et al.* 2016). So it has no adverse health impacts on the human body. Thus, it can be stated that SnO_2 is an ideal photocatalyst to work with. Few literature reports the use of pure SnO_2 nanoparticle in the photocatalysis (Singh & Nakat 2013).

Various synthetic methods are there for preparing SnO_2 nanoparticles which includes sono-chemical method (Yu *et al.* 2011), sol-gel (Lin *et al.* 2008), two-step solid state reaction (Li *et al.* 2002) and spray pyrolysis (Begum *et al.* 2016b). Precipitation method is simple, inexpensive and does not require high temperature and pressure. A huge amount of photocatalyst could be synthesized without using many reagents. Impurities in the precipitate can easily be eliminated by filtration and repeated washing (Patil *et al.* 2012; Pan *et al.* 2014; Nadaf & Venkatesh 2016).

Different research groups have synthesized SnO_2 nanoparticles and studied their applicative perspectives towards reduction and photo degradation of aromatic compounds (Begum *et al.* 2016a), photo degradation of methyl violet 6B dye and reduction of p-nitrophenol to p-aminophenol (Bhattacharjee *et al.* 2015), photocatalytic activity in methylene blue degradation (Kim *et al.* 2016), photocatalytic removal of NO gas (Huy *et al.* 2018) and degradation of carbamazepine from aqueous phase (Begum & Ahmaruzzaman 2018), etc.

4-Aminopyridine (4-AP) showed agricultural use as Avitrol and is used for repelling and killing bird pests (Takenaka *et al.* 2013). 4-AP is used by people with multiple sclerosis (Kenneth *et al.* 2000). In the laboratory of physics and biophysics, it is used in the pharmacology of various potassium conductances. But overdoses with 4-AP can lead to parenthesis, seizure and some common side effects like kidney or bladder infections, headache, nausea, weakness and back pain. The discharge of this toxic chemical as industrial effluent, agricultural, laboratory and hospital wastes contaminates the water sources. Although low in concentration, a continuous release of 4-AP, a highly stable chemical, to the aquatic environment can lead to undesirable effects causing harm to aquatic life and human health (Ljubas *et al.* 2018).

In the past few decades, advanced oxidation processes (AOPs) including semiconductor powders as photocatalysts have been engaged to treat a variety of industrial wastewaters carrying a number of products such as dyes, plastics, resin, pharmaceuticals, pesticides, etc. (ChangSong *et al.* 2000; Taib & Sorrell 2007; Saleh & Gupta 2012). Recently, researchers have focused their attention to apply semiconductor nanomaterials for the degradation of these water contaminating industrial wastes under the irradiation of UV light, visible light or even under solar light (Regmi *et al.* 2018).

Previous study reports that Fenton and photo-Fenton degradation process has been applied for removal of 3-aminopyridine (Karale *et al.* 2014). There is only a report demonstrating degradation of 4-AP using bulk ZnO photocatalyst (Chakraborty *et al.* 2017).

To the best of our knowledge, there are no previous reports focused on the photocatalytic application of synthesized SnO_2 nanoparticle towards the degradation of 4-AP under UV irradiation and solar light irradiation separately.

EXPERIMENTAL

Materials

Analytical reagent (AR) grade chemicals such as tin dichloride dihydrate ($SnCl_2.2H_2O$) and ammonia (Merck, India), were used for synthesis of SnO_2 nanoparticles without any further purification. 4-AP of 99.9% purity was purchased from Sigma Aldrich, India. The double distilled water was used as a solvent during the reaction process.

Synthesis of SnO_2 nano-powders

In the typical synthesis process, at first 2 g (0.1 M) stannous chloride dihydrate ($SnCl_2.2H_2O$) was dissolved in 100 mL water, when the pH of the solution was found to be acidic ($pH = 3$). Complete dissolution was followed by addition of 4 mL ammonia solution to the above aqueous solution with magnetic stirring. Nonstop stirring was continued for 20 min. Immediately, white gel precipitate was formed. It was allowed to settle for 12 h. Then it was filtered and washed with water 2–3 times by using deionized water. The obtained precipitate was mixed with 0.27 g carbon black powder (charcoal activated). The obtained mixer was kept in vacuum oven at 70 °C for 24 h so that the mixer turns completely in to dried powder. Then this dry product was crushed into a fine powder by grinder. Now the obtained product of fine nano-powder of SnO_2 was calcinated at 700 °C up to 6 h in the auto controlled muffle

furnace (Gayatri Scientific, Mumbai, India) so that the impurities from the product were completely removed.

Particle characterization

Optical absorption spectrum was recorded in a double beam spectrophotometer. To study the surface morphology of the prepared SnO_2 nanoparticle, field emission scanning electron microscopy (FESEM) was carried out. The crystalline phase was analyzed by X-ray powder diffraction (XRD) using Pan Analytical Expert Pro Diffractometer with copper k a radiation and a graphite monochromator to produce X-rays of wavelength 1.54 A. Diffractogram of powders were recorded in 2Θ scan configuration, in the 20–80 °C 2Θ range. Infrared spectrum was recorded in the wave number range from 500 to 4,000 cm^{-1} by Bruker Hyperion 3,000 Fourier transform infrared (FTIR) spectrometer.

Photocatalytic experiment

The photocatalysis of the synthesized SnO_2 nanoparticle observed under UV and direct sunlight was investigated by the degradation of 4-AP (5 ppm) compound analyzed spectrophotometrically at room temperature. The degradation was carried out for 2 h. For the UV irradiation, the above method was followed but a photo-reactor was designed for the UV photocatalytic activity. The reactions were conducted in a batch process in a cylindrical photo reactor with a total volume of 1.0 L (diameter 12 cm and height 13.3 cm). The catalyst (SnO_2 nanoparticle) was added to the reactor containing the sample. To house UV light ($\lambda = 240$ nm) source, the unit was set up with an annular cylindrical glass reactor consisting of a quartz tube at the center and a jacket was provided for cooling purpose. A continuous circulation of cooling media (water) was provided. The reactor was provided with inlets for intake of reactants, and outlets for collecting samples. The reactor was open to air with a magnetic stirring bar placed in the bottom for homogenization. The reactor was covered with a wooden box to prevent the exposure of UV light. Samples were periodically withdrawn for recording the absorbance of the selected compound (4-AP).

The degradation of 4-AP solution was resulted by the photocatalytic activities of synthesized SnO_2 nanoparticle. The experiments of photocatalysis were done under solar light during summer days in the month of May, in NIT Durgapur campus between 12:00 pm and 3:00 pm (atmospheric temperature 33–40 °C). Before irradiation, 500 mL aqueous solution of 4-AP (5 ppm) containing different dosage of catalyst (0.5–2 g/L) was taken in a beaker and subjected to continuous stirring in the dark for 30 min. At specified pre-selected time intervals, some aliquot of solution was taken from the solution and filtered by GF/C (25 mm) filter paper for determining the concentration, absorbance peak of 4-AP was observed at wavelength 261.5 nm using UV-Vis spectrophotometer (Shimadzu UV-1601). A standard absorbance verses 4-AP concentration calibration curve was prepared by single wavelength mode (261.5 nm) using 4-AP standard. This curve was used to determine residual 4-AP concentrations in aqueous solution at different time intervals during the photocatalytic treatment. The percentage degradation of 4-AP was calculated according to the following equation:

$$[1-(C_t/C_0)] \times 100 \quad (1)$$

where C_0 is the initial 4-AP concentration and C_t is the 4-AP concentration after photocatalytic irradiation of t minutes.

RESULTS AND DISCUSSION

XRD pattern

XRD analysis was performed to determine the size and structural properties of the synthesized SnO_2 nanoparticle. Structural identification of SnO_2 nanoparticle was carried out with X-ray diffraction in the range of angle 2 theta between 20 °C and 80 °C. Figure 1 shows the XRD pattern of synthesized SnO_2 nanoparticle formed at 700 °C which was crystalline in nature. XRD pattern showed peak at 2Θ values of 26.8 °C, 34.1 °C, 39.2 °C, 52.05 °C, 54.9 °C, 58.2 °C, 62.04 °C, 65 °C and 66.16 °C which corresponded to the (110), (101), (200), (211), (220), (002), (310), (112)

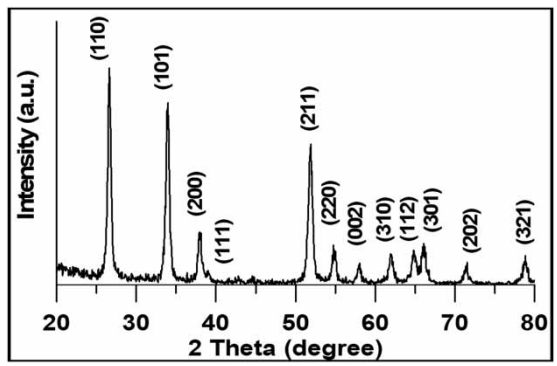

Figure 1 | XRD pattern synthesized SnO_2 nanoparticle at 700 °C.

and (301) planes respectively. The obtained peaks coincided well with previous similar observations of tetragonal rutile structure of SnO_2 nanoparticle (JCPDS 41-1445) [35].

Using Debye-Scherer's formula, the average size of the crystallite SnO_2 nanoparticle can be calculated by the equation as follows:

$$D = 0.9\lambda/\beta\cos\Theta \quad (2)$$

where the λ, the X-ray wavelength, β, the full width at half maximum of the diffraction peak (fwhm) and Θ, the Bragg diffraction angle. The average crystalline size of SnO_2 nanoparticles formed at 700 °C was calculated from the above equation and found to be 28.4 nm.

UV-Visible spectrophotometric analysis

The synthesized SnO_2 nanoparticle showing UV-Vis spectrum has been depicted in Figure 2. The figure shows that the absorption onset of SnO_2 nanoparticle was about 290 nm at 700 °C calcination temperature.

The Tauc plot was conducted to obtain the band gap energy (E_g) of semiconductor SnO_2 nanoparticles which was found to be 3.8 eV by calculating the absorption spectra. To show the relationship between the absorption co-efficient and incident photon energy, the following equation has been used:

$$\alpha(\upsilon)\, h\upsilon = K(h\upsilon - E_g)^n \quad (3)$$

where $h\upsilon$ was the incident photon energy, K, the constant, E_g, the band gap energy, α (υ), the absorption co-efficient which can be defined by the Beer-Lambert's law.

FESEM

The morphology and particle size of the prepared SnO_2 sample was determined by FESEM analysis as shown in Figure 3(a). The figure shows the FESEM picture of SnO_2 nanoparticles synthesized by using aqueous-phase method via conventional precipitation. It was observed from micrographs, particles were found to be spherical in shape and the maximum particle size distribution found in the range about 25–50 nm from Figure 3(b). The average particle size observed in both FESEM and XRD measurement was found to be nearly equal. The composition of the powders was confirmed by EDAX analysis from Figure 3(c).

FTIR

The idea of the chemical composition can be obtained from the FTIR spectra. Figure 4 has given the FTIR spectrum of SnO_2 nanoparticle. The bands acquired at around 554 cm^{-1} and 618 cm^{-1} were recognized as the Sn-O stretching modes of Sn-OH and Sn-O-Sn, respectively. The bands at around 1,630 cm^{-1} and 3,410 cm^{-1} were due to the bending vibrations of absorbed water molecule on the SnO_2 nanoparticle and the stretching vibrations of –OH, respectively. These bands were generally due to the moisture acquired during sample preparation.

Formation mechanism of SnO_2 nanoparticle

The two forms of ammonia present in water are ammonium hydroxide (NH_3) or as the ammonium ion (NH_4^+). Ammonia is present as ammonium ion when pH of the water is less than 7.

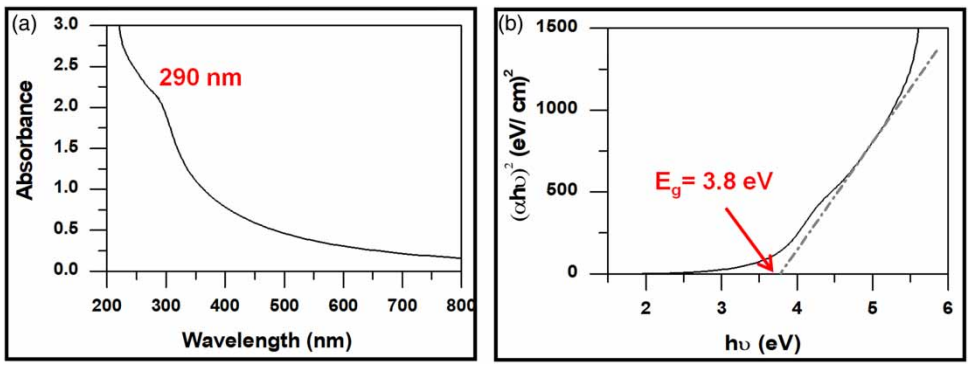

Figure 2 | (a) UV–Vis absorption spectrum of SnO_2 nanoparticles and (b) plot of $(\alpha hv)^2$ vs incident photon energy (hv) for the synthesized SnO_2 nanoparticle.

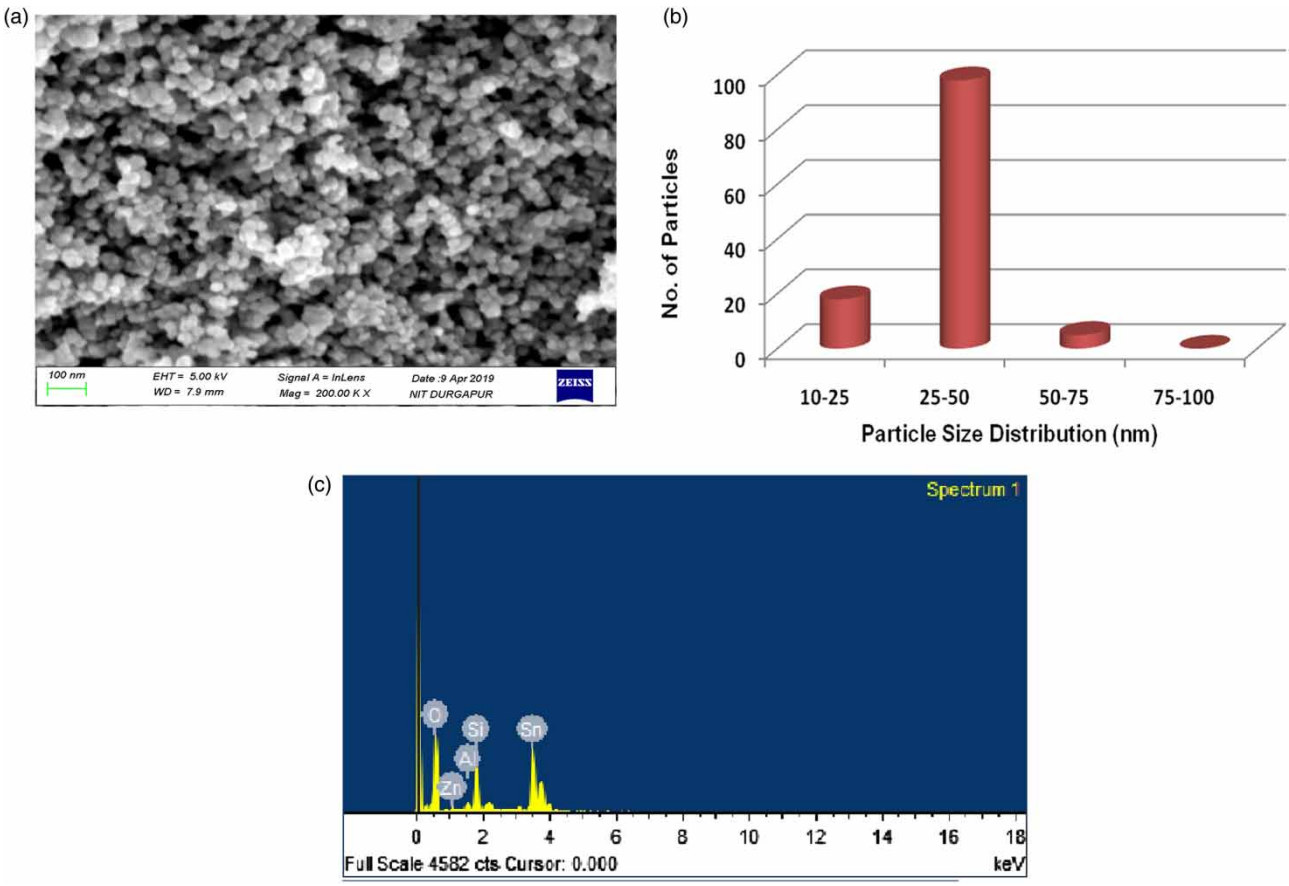

Figure 3 | (a) FESEM picture of the SnO_2 nanoparticle. (b) Particle size distribution of SnO_2 nanoparticles. (c) The composition of SnO_2 nanoparticles by EDAX analysis.

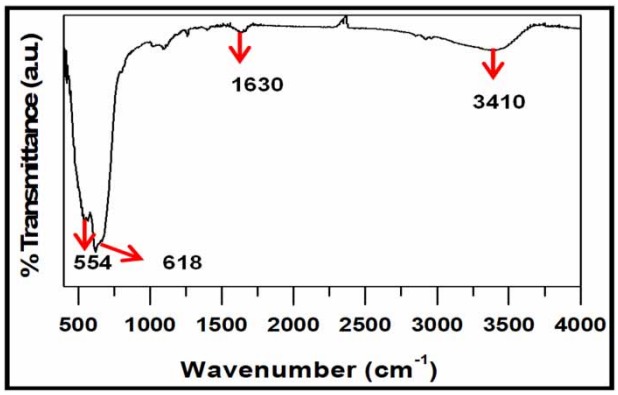

Figure 4 | FTIR spectra of synthesized SnO_2 nanoparticle.

It should be noted that when $SnCl_2.5H_2O$ was dissolved in water, the pH of the medium became acidic (pH = 3). On addition of ammonia to this solution, a milky white precipitate was formed. Ammonia played a pH adjusting role due to the formation of hydroxyl ion. The formed hydroxyl ion led to the formation of $Sn(OH)_3^-$ complex followed by the precipitation of $Sn(OH)_2$. This precipitate on annealing at 700 °C decomposed to produce SnO_2 nanoparticles.

For SnO_2 nanoparticles synthesis, the probable chemical reactions involved are as follows:

$$SnCl_2\,(s) + H_2O \longrightarrow Sn^{2+}(aq) + Cl^-(aq)$$

$$NH_3 + H_2O \longrightarrow NH_4^+ + OH^-$$

$$Sn^{2+} + 3OH^- \longrightarrow Sn(OH)_3^-$$

$$Sn(OH)_3^- \longrightarrow Sn(OH)_2 + OH^-$$

$$Sn(OH)_2 \xrightarrow{\Delta} SnO_2$$

Photocatalytic degradation of 4-aminopyridine

The degradation of toxic 4-AP water solution (5 ppm) using synthesized SnO_2 nanoparticle was studied. The catalyst

dosage and the pH were fixed at 1.5 gm/L and 6.5, respectively. In this case, UV light and direct sunlight was used as irradiation sources, separately as shown in Figure 5(i). As the illumination time increased, the degradation of 4-AP has also increased under UV light and solar irradiation both. The figure depicts the degradation rate under UV radiation was 33%, 76%, 92%, 97% and 3%, 5%, 8%, and 11% under direct sunlight.

In the solar spectrum, only 4% of UV light is present. Thus, it can be said that as the amount of UV light is very less, few upon it was absorbed for degradation. For this reason, the degradation was much lower under solar irradiation than that of UV irradiation. So, experiment under UV irradiation has been continued further but neglected under solar light.

The possible mechanism for photodegradation of 4-AP can be explained from Figure 5(ii). SnO_2 photocatalyst was excited when light with greater energy than the band gap energy was irradiated resulted in the formation of hole-electron pair in the valence band (VB) and conduction band (CB) of SnO_2 nanoparticle. Consequently, hole (h^+) may react with H_2O adsorbed on the surface of SnO_2 to form hydroxyl radicals (°OH). In the VB, photo-oxidation occurred where the holes are trapped by water molecules to form °OH. At the same time, photo-reduction also occurred where the electrons in the CB of the SnO_2 semiconductor react with dissolved molecular oxygen present in water to produce superoxide radical anion $O_2^{\circ -}$. This $O_2^{\circ -}$ reacted with H_2O to furnish °OH and HOO° having powerful oxidizing ability. The °OH is the strong oxidizing agent which helped in the degradation of the organic compound, 4-AP (Begum *et al.* 2016a).

The physico-chemical factors (like pH of the medium and catalyst dosage) that influences photocatalytic degradation has been discussed below.

Change in pH

It is believed that pH plays a key role in the photocatalytic degradation of 4-AP using SnO_2 photocatalyst. The effect of

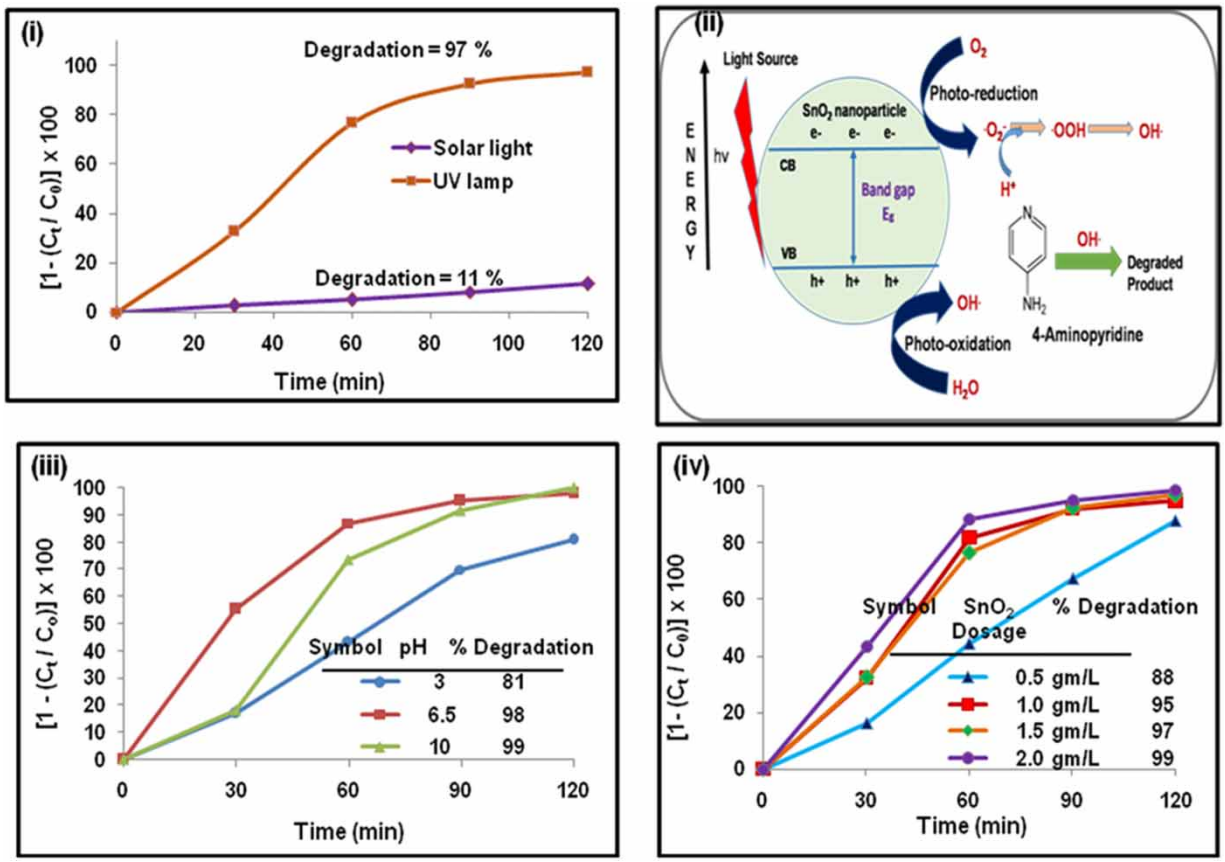

Figure 5 | (i) Photocatalytic degradation of 4-AP under UV and solar light separately, (ii) the possible mechanism for photodegradation of 4-AP, (iii) degradation of 4-AP by SnO_2 photocatalyst at varied pH, (iv) degradation of 4-AP by different dosages of SnO_2 under UV radiation.

variable pH has been shown in Figure 5(iii). The study was performed using SnO_2 dosage of 1.5 gm/L under UV light irradiation. The figure depicts catalytic degradation of 4-AP by SnO_2 at pH 3 (acidic), 6.5 (neutral) and 10 (basic) medium by adjusting the pH with the help of 0.1 M HCl or 0.1 M NaOH. The removal efficiency of 4-AP by SnO_2 was 99% at basic, 98% at neutral and 81% at acidic medium. The above results revealed that the degradation of SnO_2 in acidic pH was appreciably lower than that in the neutral as well as in the alkaline medium, which showed almost similar removal efficiency. So the degradation study had been done at neutral pH.

The influence of pH on degradation rates of 4-AP can be explained by the electrical double-layer of a solid electrolyte interface (Soltani *et al.* 2012). Under acidic condition the SnO_2 nanoparticle surface as well as 4-AP molecules were protonated (Uddin *et al.* 2016). Hence protonated SnO_2 surface hinders the adsorption of cationic 4-AP, thus explaining the lower removal efficiency in acidic pH.

Effect of catalyst dosage

To study the effect of catalyst on degradation efficiency, the SnO_2 nanoparticle with different dosage ranges from (0.5–2) gm/L was added to the 5 ppm 4-AP solution and kept under ultra-violet radiation. Figure 5(iv) shows the photocatalytic activity of SnO_2 under UV light illumination condition. The performance of the photocatalytic degradation depended immensely on the variation of catalyst loading. The degradation efficiency under catalyst dosage 0.5 gm/L, 1 gm/L, 1.5 gm/L and 2 gm/L were found to be 88, 95, 97 and 99, respectively. Up to 60 min, degradation had shown a sharp increase but after 60 min of degradation, the efficiency found to become stable. The optimum catalyst dosage was 1.0 gm/L.

This phenomenon could be explained as the low dosage of catalyst leads to the less absorption of photons by SnO_2 thereby little utilization for the photocatalytic activity. When the catalyst loading increases, the photon absorbed also increases followed by the increase in active centers on the surface of the catalyst (Hao & Jiaqiang

Table 1 | Comparison of photocatalytic degradation of targeted compound by SnO_2 nanoparticles

Catalysts (shape and particle size)	Light source	Target compound (initial conc.)	% degradation	Irradiation time (mins)	Catalyst dosage (g/L)	Reference
SnO_2 NPs (~3 nm)	7 W UV lamp, visible light $\lambda = 350$ nm Direct sunlight	MB, 10 mg/L	90.0	120	0.5	Viet *et al.* (2016)
SnO_2 NPs (15–40 nm)	Low pressure 125 W UV lamp, visible light $\lambda = 254$ nm	MB, 20 mg/L	93.3	120	2.0	Srivastava & Mukhopadhyay (2014)
SnO_2 NPs (~4 nm)	UV lamp, $\lambda = 365$ nm lamp power not determined)	Phenol red, 1 mL, 10^{-4} M	100	120	250	Elango *et al.* (2015)
Microspherical (0.4–1.8 μm diameter)	Four 8 W UV lamps (Philips UV-A, $\lambda = 350$ nm)	Aniline, (20 mg/L) 4-Nitroaniline, (20 mg/L) 2,4-Dinitroaniline (20 mg/L)	80 70 50	120	10	Talebian & Jafarinezhad (2013)
Spherical SnO_2 quantum dots (~2.5–4.5 nm)	Direct sunlight	Rhodamine B (10^{-4} M) MB (10^{-4} M)	83.9 56.8	420 360	0.05	Bhattacharjee *et al.* (2014)
SnO_2 NPs (~25–50 nm)	UV lamp, $\lambda = 240$ nm	4-Aminopyridine, 5 mg/L	97	120	1.5	This work
SnO_2 NPs (~25–50 nm)	Direct sunlight	4-Aminopyridine, 5 mg/L	11	120	1.5	This work

2010). Thus, the degradation efficiency also increased with catalyst loading.

A comparison between the present study and the previous study has been shown in Table 1. The SnO_2 nanoparticle had shown its high degradation efficiency under the UV radiation.

Reusability of the catalyst

Recycling and stability performance had been studied for SnO_2 photocatalyst. The recycling performance of catalytic efficiency was checked for three cycles (Figure 6(i)). The experimental conditions, i.e. initial concentration of pollutant solution was 5 ppm, catalyst dosage, 1.0 g/L and pH was neutral. The synthesized SnO_2 nanoparticle showed almost same degradation performance in three consecutive runs.

To check the stability of the synthesized SnO_2 photocatalyst after degradation of 4-AP in three consecutive cycles, the photocatalyst was characterized by XRD (Figure 6(ii)), FTIR (Figure 6(iii)) and FESEM (Figure 6(iv)). The figure demonstrats that there was no such change as compared to synthesized fresh SnO_2 nanoparticles.

CONCLUSION

In this paper, we developed a simple chemical precipitation method for synthesizing SnO_2 nanoparticles. The XRD pattern proved the tetragonal rutile structure of SnO_2 nanoparticles. The formation of spherical shape was evident from the FESEM images and XRD pattern. The maximum particle size distribution found in the range about 25–50 nm. The band gap energy of SnO_2 nanoparticles was obtained at 3.8 eV. The degradation efficiency of water contaminant 4-AP under UV light and solar light irradiation for 120 min were found to be 97% and 11%, respectively. These SnO_2 nanoparticles were also found to be stable photocatalysts after photocatalytic degradation. The reusability of the catalyst was checked and has been found stable after three photocatalytic runs.

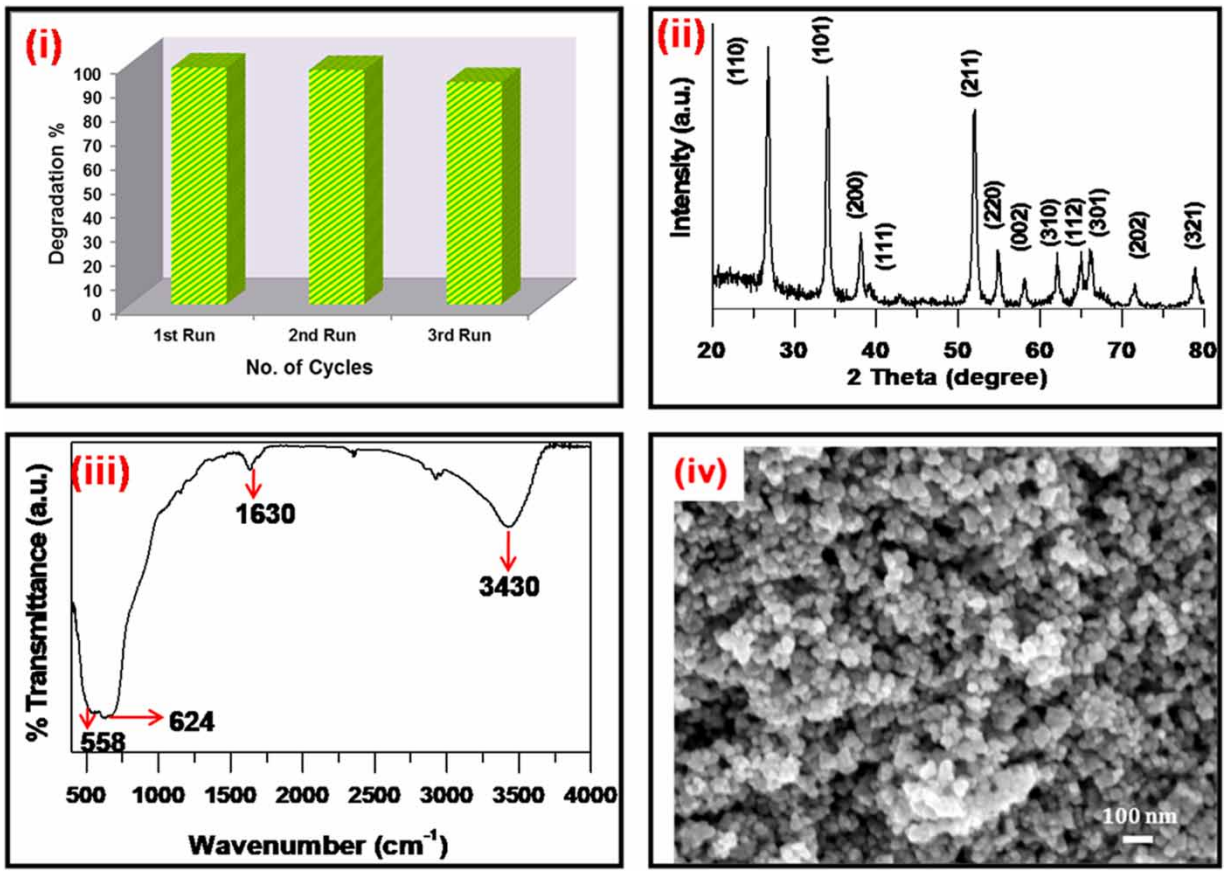

Figure 6 | (i) Bar plot representing the degradation efficiency, (ii) XRD, (iii) FTIR, (iv) FESEM of SnO_2 after photocatalytic degradation of 4-AP in three consecutive cycles.

ACKNOWLEDGEMENT

We, the authors, express our heartfelt thanks and gratitude to the Director, NIT Durgapur for providing laboratory facilities with reagents and instrumentation. Our special thanks to the department of MME for providing FESEM, XRD data and the Department of Chemistry for FTIR, spectrophotometric data. The financial support from the Department of Science and Technology under the SERB (N-PDF) sponsored project (No. PDF/2017/000390), Government of India, is gratefully acknowledged.

CONFLICT OF INTEREST

The authors declare that they have no conflict of interest.

REFERENCES

Al-Hamdi, A. M., Mika, S. & Dutta, J. 2015 Photocatalytic degradation of phenol by iodine doped tin oxide nanoparticles under UV and sunlight irradiation. *Journal of Alloys & Compounds* **618**, 366–371.

Ali, R., Abu Bakar, W. A. W., Mislan, S. S. & Sharifuddin, M. A. 2010 Photodegradation of n-methyldiethanolamine over ZnO/SnO_2 coupled photocatalysts. *Transactions C: Chemistry & Chemical Engineering* **17** (2), 24–130.

An, T., Zhang, M., Wang, X., Sheng, G. & Fu, J. 2005 Photocatalytic degradation of gaseous trichloroethene using immobilized ZnO/SnO_2 coupled oxide in a flow-through photocatalytic reactor. *Journal of Chemical Technology & Biotechnology* **8**, 251–258.

Bagheri-Mohagheghi, M. M., Shahtahmasebi, N., Alinejad, M. R., Youssefi, A. & Shokooh-Saremi, M. 2008 The effect of the post-annealing temperature on the nano-structure and energy band gap of SnO_2 semiconducting oxide nano-particles synthesized by polymerizing–complexing sol–gel method. *Physica B* **403**, 2431–2437.

Begum, S. & Ahmaruzzaman, M. 2018 CTAB and SDS assisted facile fabrication of SnO_2 nanoparticles for effective degradation of carbamazepine from aqueous phase: a systematic and comparative study of their degradation performance. *Water Research* **29**, 470–485.

Begum, S., Devi, T. B. & Ahmaruzzaman, M. 2016a L-lysine monohydrate mediated facile and environment friendly synthesis of SnO_2 nanoparticles and their prospective application as a catalyst for the reduction and photodegradation of aromatic compounds. *Journal of Environmental & Chemical Engineering* **4**, 2976–2989.

Begum, S., Devi, T. B. & Ahmaruzzaman, M. 2016b Surfactant mediated facile fabrication of SnO_2 quantum dots and their degradation behavior of humic acid. *Material Letters* **185**, 123–126.

Bhattacharjee, A., Ahmaruzzaman, M. & Sinha, T. 2014 Surfactant effects on the synthesis of durable tin-oxide nanoparticles and its exploitation as a recyclable catalyst for the elimination of toxic dye: a green and efficient approach for wastewater treatment. *RSC Advances* **4**, 51418–51429.

Bhattacharjee, A., Ahmaruzzaman, M. & Sinha, T. 2015 A novel approach for the synthesis of SnO nanoparticles and its application as a catalyst in the reduction and photodegradation of organic compounds. *Spectrochimica Acta Part A, Molecular & Biomolecular Spectroscopy* **136**, 751–760.

Chakraborty, S., Dutta, S., Saha, R., Moi, S. C., Sukul, D. & Panja, S. S. 2017 Efficacy of a photo-catalyst towards the degradation of a pharmaceutical compound, 4-aminopyridine by application of response surface methodology. *Desalination & Water Treatment* **76**, 389–397.

ChangSong, K. & Kang, Y. 2000 Preparation of high surface area tin oxide powders by a homogeneous precipitation method. *Material Letters* **42**, 283–289.

Chen, J., Li, C., Xu, F. & Zhou, Y. 2012 Hollow SnO_2 microspheres for high-efficiency bilayered dye sensitized solar cell. *RSC Advances* **2**, 7384–7387.

Elango, G., Kumaran, S. M., Kumar, S. S., Muthuraja, S. & Roopan, S. M. 2015 Green synthesis of SnO_2 nanoparticles and its photocatalytic activity of phenolsulfonphthalein dye. *Spectrochimica Acta Part A: Molecular & Biomolecular Spectroscopy* **145**, 176–180.

Hao, Y. & Jiaqiang, X. 2010 Preparation, characterization and photocatalytic activity of nanometer SnO_2. *International Journal of Chemical Engineering & Applications* **1** (3), 241–246.

Hara, K., Zhao, Z. G., Cui, Y., Miyauchi, M., Miyashita, M. & Mori, S. 2011 Nanocrystalline electrodes based on nanoporous-walled WO_3 nanotubes for organic-dye-sensitized. *American Chemical Society* **27**, 12730–12736.

Hu, M., Zhang, Z., Luo, C. & Qiao, X. 2017 One-pot green synthesis of Ag-decorated SnO_2 microsphere: an efficient and reusable catalyst for reduction of 4-nitrophenol. *Nanoscale Research Letters* **12**, 435.

Huy, T. H., Phat, B. D., Thi, C. M. & Viet, P. V. 2018 High photocatalytic removal of NO gas over SnO_2 nanoparticles under solar light. *Environmental Chemistry Letters* **17**, 527–531.

Karale, R. S., Manu, B. & Shrihari, S. 2014 Fenton and photo-Fenton oxidation processes for degradation of 3-aminopyridine from water. *APCBEE Proceedings* **9**, 25–29.

Kenneth, J. S., Paul, A. F. & Gareth, R. J. 2000 Effects of 4-aminopyridine on demyelinated axons, synapses and muscle tension. *Brain* **123**, 171–184.

Kim, S. P., Choi, M. Y. & Choi, H. C. 2016 Photocatalytic activity of SnO_2 nanoparticles in methylene blue degradation. *Material Research Bulletin* **74**, 85–89.

Li, F., Chen, L., Chen, Z., Xu, J., Zhu, J. & Xin, X. 2002 Two-step solid-state synthesis of tin oxide and its gas-sensing property. *Materials Chemistry & Physics* **73** (2), 335–338.

Li, Y., Yang, Q., Wang, Z., Wang, G., Zhang, B., Zhang, Q. & Yang, D. 2018 Rapid fabrication of SnO_2 nanoparticle photocatalyst: computational understanding and

photocatalytic degradation of organic dye. *Inorganic Chemical Frontiers* **5**, 3005.

Lin, C. F., Wu, C. H. & Onn, Z. N. 2008 Degradation of 4-chlorophenol in TiO_2, WO_3, SnO_2, TiO_2/WO_3 and TiO_2/SnO_2 systems. *Journal of Hazardous Materials* **15**, 1033–1039.

Lin, Y. M., Nagarale, R. K., Klavetter, K. C., Heller, A. & Mullins, C. B. 2012 SnO_2 and TiO_2-supported-SnO_2 lithium battery anodes with improved electrochemical performance. *Journal of Material Chemistry* **22**, 11134–11139.

Ljubas, D., Cizmic, M., Vrbat, K., Stipanicev, D., Repec, S., Curkovic, L. & Babic, S. 2018 Albendazole degradation possibilities by UV-based advanced oxidation processes. *International Journal of Photoenergy*. Article ID 6181747.

Nadaf, L. I. & Venkatesh, K. S. 2016 Synthesis and characterization of Tin oxide nanoparticles by Co-precipitation method. *IOSR Journal of Applied Chemistry* **9**, 01–04.

Pan, R., Wu, Y., Li, Z. & Fang, Z. 2014 Effect of irradiation on deposition of CdS in fabrication co-axial heterostructure of TiO_2 nanotube arrays via chemical deposition. *Applied Surface Science* **292**, 886–891.

Patil, G. E., Kajale, D. D., Gaikwad, V. B. & Jain, G. H. 2012 Preparation and characterization of SnO_2 nanoparticles by hydrothermal route. *International Nano Letters* **2**, 17.

Prakasha, K., Senthil, K. P., Pandiarajb, S., Saravanakumara, K. & Karuthapandian, S. 2016 Controllable synthesis of SnO_2 photocatalyst with superior photocatalytic activity for the degradation of methylene blue dye solution. *Journal of Experimental NanoScience* **11** (14), 113–1155.

Regmi, C., Joshi, B., Ray, S. K., Gyawali, G. & Pandey, R. P. 2018 Understanding mechanism of photocatalytic microbial decontamination of environmental wastewater. *Frontiers in Chemistry* **6**, 33.

Saleh, T. A. & Gupta, V. K. 2012 Column with CNT/magnesium oxide composite for lead (II) removal from water. *Environmental Science & Pollution Research* **19**, 1224–1228.

Singh, A. K. & Nakat, U. T. 2013 Microwave synthesis, characterization and photocatalytic properties of SnO_2 nanoparticles. *Advances in Nanoparticles* **2**, 66–70.

Soltani, N., Saion, E., Hussein, M. Z., Erfani, M., Abedini, A., Bahmanrokh, G., Navasery, M. & Vaziri, P. 2012 Visible light-induced degradation of methylene blue in the presence of photocatalytic ZnS and CdS nanoparticles. *International Journal of Molecular Science* **13**, 12242–12258.

Srivastava, N. & Mukhopadhyay, M. 2014 Biosynthesis of SnO_2 nanoparticles using bacterium *Erwinia herbicola* and their photocatalytic activity for degradation of dyes. *Industrial & Engineering Chemical Research* **53** (36), 13971–13979.

Taib, H. & Sorrell, C. C. 2007 Preparation of tin oxide. *Journal of the Australian Ceramic Society* **43**, 56–61.

Takenaka, S., Nomura, R., Minegishi, A. & Yoshida, K. 2013 Enrichment and characterization of a bacterial culture that can degrade 4-aminopyridine. *BMC Microbiology* **13**, 62.

Talebian, N. & Jafarinezhad, F. 2013 Morphology-controlled synthesis of SnO_2 nanostructures using hydrothermal method and their photocatalytic applications. *Ceramics International* **39**, 8311–8317.

Tripathy, S. K., Mishra, A., Jha, S. K., Wahab, R. & Al-Khedhairy, A. A. 2013 Microwave assisted hydrothermal synthesis of mesoporous SnO_2 nanoparticles for ethanol sensing and degradation. *Journal of Materials Science: Materials Electronics* **24**, 2082–2090.

Uddin, M. T., Sultana, Y. & Islam, M. A. 2016 Nano-sized SnO_2 photocatalysts: synthesis, characterization and their application for the degradation of methylene blue dye. *Journal of Scientific Research* **8**, 399–411.

Viet, P. V., Thi, C. & Hieu, L. V. 2016 The high photocatalytic activity of SnO_2 nanoparticles synthesized by hydrothermal method. *Journal of Nanomaterials* **8**, Article ID 4231046.

Yu, Z., Zhu, S., Li, Y., Liu, Q., Feng, C. & Zhang, D. 2011 Synthesis of SnO_2 nanoparticles inside mesoporous carbon via a sonochemical method for highly reversible lithium batteries. *Material Letters* **65**, 3072–3075.

First received 16 August 2019; accepted in revised form 13 March 2020. Available online 23 March 2020